ELSEVIER

Chemical Physics 233 (1998) 353–363

Chemical Physics

Wavepacket diagnosis with chirped probe pulses

R. Zadoyan *, N. Schwentner [1], V.A. Apkarian

Department of Chemistry, University of California, Irvine, CA 92697, USA

Received 29 January 1998

Abstract

For linearly chirped probe pulses, the observable pump–probe signal can be obtained analytically under useful idealizations: Gaussian packet and pulse, linear chirp, linear difference potential, and constant wavepacket group velocity within the probe window. These conditions allow the expression of the signal as a cross correlation between packet and probe window traveling in coordinate space at velocities v and v_l, respectively. The signal delay and its integrated area are independent of chirp. Relative to zero-chirp, the signal is temporally compressed for $0 < v/v_l < 2$, and becomes a minimum when packet and window co-propagate, $v = v_l$. Experimental data are used to illustrate wavepacket diagnosis in a real system.

Keywords: Wavepacket diagnosis; Chirped probe pulses; Probes

1. Introduction

Time resolved measurements in the ultrafast domain necessarily involve two pulses: a pump-pulse, which prepares an initial nonstationary superposition state, or a wavepacket; and a probe-pulse, which interrogates the packet after some time evolution. Many theoretical models, ranging from classical [1,2], to generalized linear response [3,4], to semi-classical [5], and rigorous nonlinear spectroscopic analyses [6], have been developed to describe the pump–probe process. Since ultrashort pulses are used in such measurements, the spectral bandwidths are non-negligible. The observable signal will then depend on the joint time–frequency profile of pulses, or equivalently the coherences of the radiation fields employed, which can most generally be described through the chrono-cyclic representation [7]. An understanding of the dependence of the observable signal on the frequency sweep, or chirp, in the probe pulse is useful for the most mundane of considerations: pulses used in measurements are seldom transform limited. More to the point, low order chirp, which can easily be manipulated and measured, gives an added tool for the characterization of the evolving packet. In fact, since the coordinate-time distributions of wavepackets and probe pulses are usually comparable, the dependence of observable signals on the controlled coherence of the probe is the only means to characterize the coherence of the evolving packet. With experiments in condensed phase in mind [8], the effect of linear chirp on observables

* Corresponding author.

[1] Permanent address: Institut für experimentalphysik, Freie Universität Berlin, Arnimallee 14, D-14195 Berlin, Germany.

0301-0104/98/$19.00
PII: S0301-0104(98)00170-0

has been addressed through numerical simulations using classical molecular dynamics and a classical representation of the matter–radiation interaction [9]. A clear physical insight on the effect of probe chirp can be obtained when transforming the ω–t distribution of the pulse into the r–t plane, and noting that the window function thus generated acquires velocity when the pulse is chirped [8,9]. The relative group velocity between packet and probe window determines the observable signal. Cao and Wilson [10] have given more generalized treatments of the same physics, through semiclassical and classical analysis. Beside noting the general validity of the classical treatment [10,11], which is inappropriate when pump and probe pulses overlap, they also recognized that the probe pulse itself prepares yet another state, a final state, the coherence of which may be controlled by the evolving packet and the probe-pulse chirp [10–13]. From this point of view of coherence control using chirped pulses, a significant body of work has emerged from Wilson's group, most recently using three-photon absorption [14]. In short, detailed analyses at different levels of theoretical rigor exist on the subject. Nevertheless, it is useful to consider conditions which lead to an analytical solution of the problem, to obtain a simple statement of the effect of probe chirp and its utility in the diagnosis of wavepacket evolution.

We will consider the pump–probe experiment illustrated in Fig. 1. The pump-pulse prepares a packet on the electronic potential surface identified as V_2. The probe-pulse, characterized with the spectral distribution $\delta\omega$, is resonant with the $V_3 \leftarrow V_2$ transition. The projection of this spectral distribution on coordinate space is obtained by reflection through the difference potential, $\Delta V = V_3 - V_2$ [9]. This defines the probe window, as a spatial distribution, δx, in coordinate space (see Fig. 1). The probe intensity is assumed weak, such that only a small fraction of the packet is promoted to the final state when the packet crosses the window. The population created on the final state is then detected, possibly, through fluorescence. The fluorescence, as a function of delay between pump and probe defines the observable signal, $S(t)$. We are interested in the dependence of the time profile of $S(t)$ on probe chirp, namely on the ω–t distribution of the probe-pulse. Given that the probe pulse width is shorter than any recursions on either V_2 or V_3, the probe absorption may be treated classically. This has been used in our earlier numerical analysis of pump–probe signals using chirped pulses [9], and has been shown to agree quantitatively with experiment [8,15], semi-classical and quantum treatments [10–16]. Note, rather than fields, in the classical treatment one only needs a description of the intensity-power spectrum of the laser pulse [9]. An example of a positively chirped pulse, and its reflection through the difference potential, is shown in Fig. 2. The slope of the pulse profile in ω–t space generates a slope in x–t space: the probe window acquires velocity v_l (negative in this case). The wavepacket of Fig. 1 is shown in the x–t plane in Fig. 2 to have a positive velocity v. Quite clearly, the observable signal is the joint space-time overlap of the traveling packet and traveling window. The signal will therefore depend on the x–t profile of the probe window, which in turn can be tilted by tilting the axis of the pulse represented in the ω–t plane. A simple solution is obtained when the packet and window are described as Gaussians traveling with constant velocity. We give the explicit steps

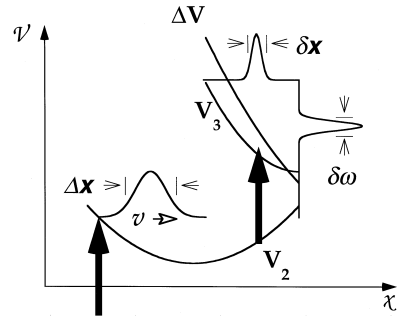

Fig. 1. Schematic of the pump–probe experiment. A packet is prepared on V_2 using the pump pulse. It evolves with a group velocity v. The packet is probed with a pulse resonant with the $V_3 \leftarrow V_2$ transition. The spectral width of the probe pulse, $\delta\omega$, defines the width of the probe window in coordinate space, δx, by reflection through the difference potential $\Delta V = V_3 - V_2$.

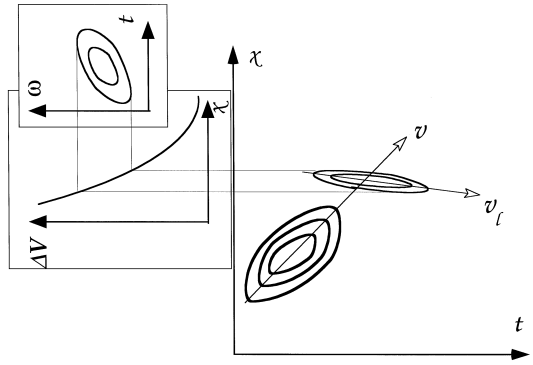

Fig. 2. Transformation of the probe pulse from $\omega - t$ plane to $x - t$ plane, and definitions of packet velocity, v, and window velocity, v_l.

below, and discuss the implications. We follow this by an implementation that goes beyond the strict limits of the analytical theory.

2. Analytical limit

The observable signal in a pump–probe experiment, including chirp in the pulses used, can be determined analytically under the simplifying assumptions that both wavepacket and probe window are given as constant velocity traveling Gaussians. Assume that the wavepacket prepared with an ultra-short pump pulse, $\rho(x,t)$, at the time of its interrogation, t', is well described as a Gaussian traveling with a group velocity v:

$$\rho(x;t') = \frac{1}{\sqrt{2\pi}\,\Delta x} \exp\left[-\frac{(x - vt')^2}{2\Delta x^2}\right]. \tag{1}$$

It will be useful to transform this to t-space, by using $x = vt$, and conserving normalization, $\rho(t) = \rho(x)\mathrm{d}x/\mathrm{d}t$:

$$\rho(t) = \frac{1}{\sqrt{2\pi}\,\Delta t} \exp\left[-\frac{(t - t')^2}{2\Delta t^2}\right]. \tag{2}$$

Assume that the probe pulse has a Gaussian time profile in intensity, and therefore a Gaussian power spectrum. Then a linearly chirped probe pulse may be expressed as [9]:

$$I(\omega,t;\tau) = \frac{1}{\sqrt{2\pi}\,\delta\omega\delta t} \exp\left[-\frac{(\omega - \omega_0)^2}{2\delta\omega^2} - \frac{\left(t - (\tau + \alpha(\omega - \omega_0))\right)^2}{2\delta t^2}\right] \tag{3}$$

where α, which corresponds to the slope of the Gaussian pulse in the ω–t plane, represents the chirp of the probe pulse and may be positive or negative. Using the difference potential of the probe transition, and noting the vertical nature of optical transitions, it is possible to transform the probe pulse distribution to the x–t plane, to generate the window function, $W(x,t)$:

$$I(\omega,t;\tau) \overset{\delta[\hbar w - \Delta V]}{\rightarrow} W(x,t;\tau). \tag{4}$$

This is simply a restatement of the classical Franck principle for optical transitions. The difference potential, at the probe resonance, may be expanded in a Taylor series. Assuming that in the limited range of the probe

window the difference potential can be represented as a linear function, so that we may limit the expansion to the linear term:

$$\frac{\Delta V(x)}{\hbar} = V_0 + V_1 x + \ldots \tag{5}$$

the probe window function may be written explicitly:

$$W(x,t;\tau) = \frac{1}{\delta x \delta t \sqrt{2\pi}} \exp\left[-\frac{(x-x_0)^2}{2\delta x^2} - \frac{\left(t-\left(\tau+\alpha V_1(x-x_0)\right)\right)^2}{2\delta t^2} \right]. \tag{6}$$

Recall that α is the tilt of the Gaussian probe pulse in ω–t (units of fs/cm^{-1}), V_1 is the local slope of the difference potential (cm^{-1}/Å), and αV_1 represents the tilt of the Gaussian window in x–t plane (in units of fs/Å). We recognize that if the window function has a slope in x–t plane then the probe window has a velocity:

$$v_1 = \frac{1}{\alpha V_1}. \tag{7}$$

This is the velocity acquired due to the chirp of the probe pulse. In the case of zero-chirp, $\alpha = 0$, the red and blue edges of the probe pulse arrive simultaneously, therefore the window is spanned instantaneously, or $v_1 \to \infty$.

Save for a proportionality constant related to transition strength, the observable signal at a given time, $S(t)$, is determined by the space–time overlap of the packet and window:

$$S(\tau) = \int \mathrm{d}x \int \mathrm{d}t \rho(x,t) W(x,t;\tau) = \frac{1}{(2\pi)^{3/2} \Delta x \delta x \delta t} \int \mathrm{d}x \exp\left[-\frac{(x-x_0)^2}{2\delta x^2} \right] \int \mathrm{d}t \exp\left[-\frac{(x-vt)^2}{2\Delta x^2} \right]$$
$$\times \exp\left[-\frac{\left(t-\left(\tau+\alpha V_1(x-x_0)\right)\right)^2}{2\delta t^2} \right]. \tag{8}$$

These Gaussian integrals can be evaluated analytically, to obtain a normalized Gaussian as the signal at time τ:

$$S(\tau) = \frac{1}{\sqrt{2\pi}\,\gamma} \exp\left[-\frac{(x_0 - v\tau)^2}{2\gamma^2} \right] \tag{9}$$

where

$$\gamma^2 = v^2 \delta t^2 + \Delta x^2 + \delta x^2 \left(1 - \frac{v}{v_1} \right)^2 \tag{10}$$

and the integrated area of the signal is determined solely by the packet velocity:

$$S = \int S(\tau) \mathrm{d}\tau = \frac{1}{v}. \tag{11}$$

The first important conclusion is that the integrated signal is independent of chirp, with the important consequence that in this sequential excitation scheme, the net population transferred to the final state is conserved. Secondly, according to Eq. (9), the signal peak occurs at $\tau = x_0/v$, namely at the time of arrival of the packet to the fixed center of the probe window, x_0, independent of chirp. The probe chirp, however, does

change the time profile of the signal, and therefore the space–time distribution, or the coherence, of the preparation on the final surface [10–13]. Consider the temporal width of the signal by recasting Eq. (10) as:

$$\gamma_t^2 = \gamma^2/v^2 = \delta t^2 + \Delta t^2 + \delta x^2 \left(\frac{1}{v} - \frac{1}{v_1} \right)^2 . \tag{12}$$

This form lends itself to the most direct physical interpretation, by considering the propagation of the packet and the window in the x–t plane. Nevertheless, it is useful to also write the same in terms of characteristic experimental observables:

$$\gamma_t^2 = \delta t^2 + \Delta t^2 + \delta \omega^2 \left(\frac{1}{vV_1} - \alpha \right)^2 . \tag{13}$$

The experiments measure the temporal width of the pump–probe signal, γ_t. The probe pulse width, δt, its chirp, α, and spectral width, $\delta\omega$, are determinables, from an independent measurement, e.g., through frequency resolved optical gating (FROG) of the probe pulse [17]. In cases where the spectroscopy of the system is well at hand, the probe difference potential characterized by V_1 may also be independently known. More often, and in particular in the case of multi-dimensional systems, the difference potential is to be characterized along with the retrieval of the evolving packet. The evolving packet is the main target of the experiment, and here, it is to be characterized by its width, Δt, and instantaneous group velocity, v. Note that at early time, before the dispersion of the prepared wavepacket, Δt will be dominated by the pump pulse width, Eq. (2). With this in mind, it may be recognized that Eq. (12) corresponds to the response function of a cross-correlator by identifying δx with the correlator crystal thickness, and v and v_l with the group velocities of pulses that arise from dispersion in the correlator (see for example [18]).

Now consider the effect of chirp on the observable signal width by specifying the conditions implied by Eq. (12) (or Eq. (13)). At zero chirp, the temporal width of the signal is the geometric average of the widths of the packet, the probe pulse, and the time for passage of the packet through the probe window:

$$\gamma_0 = \left\{ \delta t^2 + \Delta t^2 + \delta x^2/v^2 \right\}^{1/2}, \text{ for } v_1 = \infty \ (\text{or } \alpha = 0) . \tag{14}$$

The minimum width of the signal, which is narrower than the zero-chirp response, is obtained when the window and packet co-propagate with the same speed (this is the desirable configuration of the cross-correlator):

$$\gamma_{\min} = \left\{ \delta t^2 + \Delta t^2 \right\}^{1/2}, \text{ for } v = v_1 \ (\text{or, for } \alpha = 1/vV_1) \tag{15}$$

and clearly, the response function may not be narrower than the cross-correlation between pump and probe.

The condition for observing a signal narrower than that at zero-chirp is:

$$\gamma_t < \gamma_0, \text{ for } 0 < v/v_1 < 2 \ (\text{or, for } 0 < \alpha v V_1 < 2) . \tag{16}$$

Equivalently, when the packet and window counter-propagate, $v/v_l < 0$ (or $\alpha v V_1 < 0$), the signal response is always broader than that at zero-chirp. The same is also true when $v_l > v/2$. These conditions follow from the fact that in Eq. (12), the broadening of the response of the correlator is determined by the reduced relative velocity of propagation through the window, $|(v - v_l)/vv_l|$.

The diagnostic value of measurements as a function of probe chirp should be obvious from the above. In the case where the probe difference potential, therefore V_1, is independently known, by varying the probe chirp rate, α, the evolving packet can be fully characterized. A possible procedure may be the determination of the chirp that yields the narrowest time response. Then, from the measured value of α, the instantaneous velocity of the packet (its magnitude and direction) are determined, since at $\gamma_{\min}$; $v = v_l = 1/\alpha V_1$. Moreover, from the measured signal width and the known probe pulse width, according to Eq. (14), the spread of the packet in time, Δt, or space, $\Delta x = v\Delta t$, is determined. If, however, V_1 is not known, then measurements as a function of probe chirp alone are not sufficient to characterize both the packet and the difference potential. This should be evident

from Eq. (13), in which only the product vV_1 appears as an independently determinable variable. In this context, it is also important to note that directions of propagation are relative to the difference potential gradient. To be concrete, if α were adjusted to minimize the observed signal width, based on the sign of the chirp we may only learn that the packet travels along or opposite the slope of the difference potential. In the case of multidimensional potential energy surfaces, the analysis is further complicated since packet and window do not necessarily evolve along the same coordinate [19]. Even in the one-dimensional case additional input is required to fully retrieve the wavepacket and to simultaneously characterize the difference potential. Either measurements at different probe wavelengths, or in subsequent recursions of the packet to the same window, can enable such a retrieval.

3. Experimental

The experiments that inspired the earlier numerical treatments [8,9], fall outside the limits of strict applicability of the analytical solutions. Nevertheless, they serve as a useful illustration of what can be learned from a blind experiment. The measurements consist of preparing $I_2(A)$ in solid Kr, using the fundamental output of a Ti: Sapphire laser at 792 nm. The doubled output of the Ti:Sapphire laser, which is resonant with the $\beta \leftarrow A$ transition is used as probe, and the fluorescence from the ion-pair manifold is used as monitor. The pulses are characterized by frequency resolved optical gating (FROG), using the Kerr effect in the polarization gate geometry [17]. A 1 mm thick quartz substrate is used to characterize the pump pulse in auto correlation, and a 100-μm glass substrate is used to characterize the probe pulse by cross-correlation. The gated pulses are dispersed in a 1/4-m polychromator, and detected using a 1024-element intensified diode array (OMA III). The

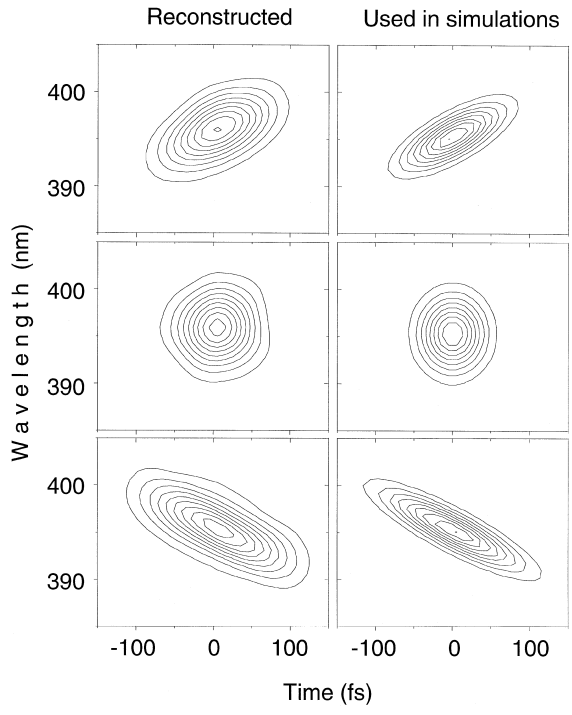

Fig. 3. Profiles of the probe pulses used in the experiment as retrieved from the FROG data, and their representation as single Gaussians, according to Eq. (3) of text. Note axes are λ and t, accordingly from top to bottom the panels represent negative, zero, and positive chirp.

gated spectra are then used to reconstruct the pulses using software (FROG 1.5, Femtosecond Technologies) which has been described in the literature [17]. Assuming a normal Gaussian, the pump pulse width is $\Delta t = 25.5$ fs (HWHM = 30 fs), and it is adjusted for zero-chirp using an external compensator consisting of two BK-7 prisms. The probe pulses used in the experiment are illustrated in the λ–t plane in Fig. 3, where the retrieved intensity distributions along with their single Gaussian representation according to Eq. (3) are given. The probe pulse parameters of Eq. (3), are: $\delta t = 28$ fs, $\delta\omega = 298$ cm^{-1}, for the positively chirped pulse $\alpha = 0.298$ fs/cm^{-1}, and for the negatively chirped pulse $\alpha = -0.219$ fs/cm^{-1}. The probe chirp is controlled by a separate two-prism compensator using fused silica prisms. Relatively small frequency sweeps are used to avoid nonlinearities. Clearly, the Gaussian representation of the pulses is an approximation.

4. Results and analysis

The observed signal consists of two distinct resonances due to interception of the packet during its outbound stretch, and during its recoil after collision with the cage (for further details see Refs. [9] and [19]). Along with the experimental data in Fig. 4 we also provide strictly numerical reconstructions of the observable signal. These are extracted from molecular dynamics simulations, and are based on 60 trajectories in a cell containing 500

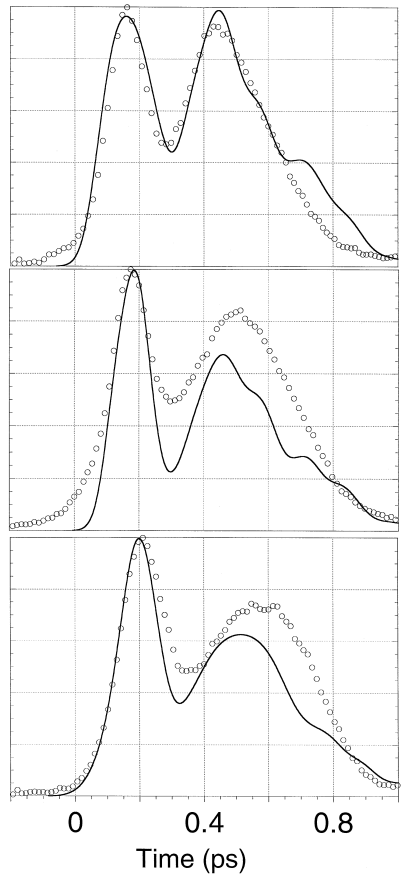

Fig. 4. The observed experimental signal (open circles) and simulated signal using trajectory data and one-dimensional inversion (solid line) for the three probe pulses shown in Fig. 3.

atoms with periodic boundary conditions. The trajectory data in this case is inverted to signal under the assumption of a probe window fixed along the molecular coordinate [9,19]. Thus, although the dynamics is propagated in full dimensionality, the inversion is in effect in one-dimension, and does not take into account the modulation of the ion-pair state due to evolution on the intermediate A state. Despite this approximation the simulations reproduce the general features of the signal. Most notably, the trend in relative intensities of the two resonances as a function of chirp is reproduced. Note, the measurements do not yield an absolute time origin. We have adjusted the amplitude and time origin of the first experimental peak to match with the simulation.

The first clue to the failure of the assumptions of the analytical model is the fact that the peak positions depend on chirp. Fig. 4 illustrates that as we proceed from positive to negative chirp, the relative separation between the two resonances is reduced. This is captured in the numerical simulations, which indicate that both resonances move to earlier time. In the simulations the probe resonance occurs near the minimum of the difference potential, a region which is dominated by the quadratic term in the Taylor expansion rather than the linear term to which we limited Eq. (5). Accordingly, the window function in r–t space acquires a quadratic chirp [9]. Moreover, it is possible to verify that the recoiling packet undergoes significant acceleration while within the resonance window. Thus, the assumption of a constant group velocity within the probe window does not hold. Nevertheless, the data can be rationalized by approximating the quadratic difference potential near its minimum by two linear windows, one on either side of the potential minimum, and by recognizing that the outer window with its positive slope will dominate, since the packet is slowest there and since this side of the difference potential has a softer slope. The shift in peak positions as a function of probe chirp can then be understood to arise from differential weighting of contributions from windows with opposite linear slopes, and four contributions in all (two for outgoing wavepacket, and two for returning packet). Quite clearly the data can be fit by four Gaussians. The three sets of data, with probe laser parameters, δt, $\delta\omega$, and α, fixed by the FROG measurements, constrain a unique decomposition under this assumption. This constrained fit is shown in Fig. 5, and is accomplished as follows:

(a) An initial packet velocity is chosen for the outbound wave, and assumed to be constant through both windows. The initial guess of this velocity was based on trajectory data, $v = 5.5$ Å/ps, and could not be improved by iteration.

(b) Based on the fact that in the experiment the area under the second peak is nearly twice that of the first, according to Eq. (11), the velocity of the returning packet must be nearly half the original. The data imposes the assumption of acceleration during recoil, by assuming different velocities under the two windows for the returning packet. The values used after some iteration are: $v_r = 2$ Å/ps and $v_l = 2.8$ Å/ps, for the right and left windows, respectively. Note, the velocities determine the areas, therefore, the heights of the Gaussians.

(c) The window parameters consist of choosing slopes for the difference potentials, for which $V_l = -1500$ cm^{-1}/Å and $V_r = 1100$ cm^{-1}/Å are accepted after some iteration. These choices are highly constrained by the choice of velocities, since the product vV is inseparable in the expressions for $S(t)$.

(d) The location of the windows reduces to the choice of the centers of the Gaussians, which are simply adjusted to obtain the best fit for the full data set.

(e) The width of the outbound packet, Δt, is initially assumed to be the same as the pump pulse width. A better fit is obtained with the assumption of some broadening, $\Delta t = 30$ fs in both windows during the outbound stretch. The width of the recoiling packet is taken as a variable, and determined as $\Delta t = 95$ fs, assumed to be the same in both windows during recoil.

The decomposition shown in Fig. 5 shows clearly the origin of peak shifts with chirp. The contribution of the two windows to the first peak is the more obvious, since here the velocity of the packet is constant. In the outbound stretch the velocity of the packet is positive, $v > 0$; since the slope of the first window is negative, while that of the second is positive, then for a negatively chirped pulse, the window co-propagates with the packet, $v_l > 0$ in the first window, and counter-propagates in the second window, $v_l < 0$. Accordingly, for the negatively chirped pulse the width γ of the response function is narrower, and therefore the peak higher, in the first window, and shorter in the second window. These arguments are reversed for the positively chirped pulse.

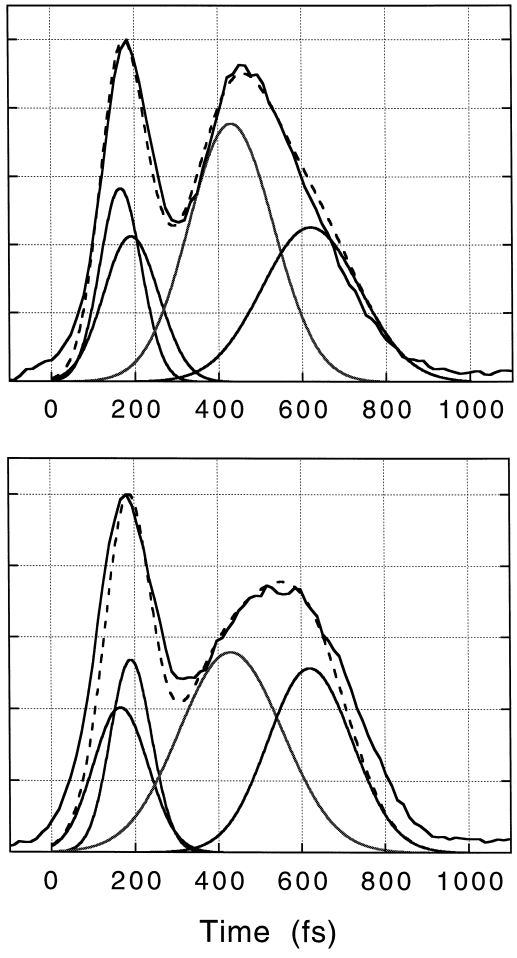

Fig. 5. Gaussian decomposition of the data as suggested by the analytical solutions, and based on the assumptions of two windows: top panel-negative chirp, bottom panel-positive chirp.

The same rationale prevails in the case of the second peak, but now for the recoiling packet which has a negative velocity. However, since the packet accelerates between windows in this case, the contributions from each window do not fully invert (as they do in the case of the first peak) when the chirp is reversed.

The analysis also yields an important insight regarding the nonstationary nature of probe windows in multi-dimensional systems. The centers of the Gaussians yield the arrival time of the packet to the effective center of the window. Since the velocity is constant in the first passage, we can extract the implied separation between windows as 0.137 Å (difference in crossing times of 25 fs). If we use the mean velocity for the recoiling packet, the separation between the same two windows is obtained as 0.45 Å (difference in crossing times of 190 fs). The implication is that after collision of the I atoms with the cage, upon setting the lattice coordinates into motion, due to the differential solvation of the ion-pair state and the covalent A state, the difference potential evolves in time. This indeed should occur, yet such effects are not contained in numerical simulations that rely on one-dimensional inversion of trajectory data. Thus, as expected, the diagnosis of the packet yields information about not only dynamics evolving on the prepared state, but also the time evolution of

the final state. In effect, the present treatment is less biased than numerical simulations that make assumptions about the difference potential.

5. Conclusions

Probe chirp dependence of pump–probe signals provides a powerful means for the diagnosis of wavepackets. We have presented an analytical treatment of the effect of probe chirp on observable signal, which is rigorously valid under special conditions: linear chirp, linear difference potential, and constant wavepacket group velocity within the probe window. The treatment yields a simple intuitive picture for the effect of chirp on observable signals, or on coherences prepared by sequential excitation. The analysis remains useful in interpretations of data, through multiple Gaussian decompositions, when the strict conditions of validity of the analytical solutions are not held. We have demonstrated this in the case of the multidimensional wavepacket dynamics of I_2 isolated in solid Kr, a system that had already been considered through purely numerical simulations [9]. The unbiased characteristics of the packet, its initial momentum, momentum after collision with the cage, acceleration after recoil, and its dispersion during propagation, are in good agreement with the trajectory data. Additionally, the Gaussian decomposition uniquely establishes that the probe window is not stationary along the molecular coordinate, yielding information about the differential solvation of electronic states used for the probe transition. Specifically, the analysis locates the difference potential through its position and first derivative at resonance, without prior information.

The presented treatment is also useful in predicting coherences prepared by chirped pulses, and can easily be extended to multi-photon processes.

Acknowledgements

We gratefully acknowledge the support by AFOSR, under a University Research Initiative grant F49620-1-0251, which made this work possible. N.S. acknowledges financial support provided by the UCI Institute for Surface and Interface Studies (ISIS) during his stay at Irvine. We also acknowledge the general inspiration provided through our collaboration with K.R. Wilson and his group regarding control of wavepacket dynamics with chirped pulses.

References

[1] R. Bersohn, A.H. Zewail, Ber. Bunsenges. Phys. Chem. 92 (1988) 373.
[2] R.E. Walkup, J.A. Misewich, J.H. Glownia, P.P. Sorokin, Phys. Rev. Lett. 65 (1990) 2366.
[3] B. Fain, S.H. Lin, N. Hamer, J. Chem. Phys. 91 (1989) 4485.
[4] W.T. Pollard, S.-Y. Lee, R.A. Mathies, J. Chem. Phys. 92 (1990) 4012.
[5] Y.J. Yan, L.E. Fried, S. Mukamel, J. Phys. Chem. 1989 (1989) 8149.
[6] Y.J. Yan, S. Mukamel, Phys. Rev. A 41 (1990) 6485.
[7] J. Paye, IEEE J. Quant. Electron. 28 (1992) 2262.
[8] V.A. Apkarian, in: M. Chergui (Ed.), Femtochemistry, World Scientific, Singapore, 1996, p. 603.
[9] M. Sterling, R. Zadoyan, V.A. Apkarian, J. Chem. Phys. 104 (1996) 6497.
[10] J.S. Cao, K.R. Wilson, J. Chem. Phys. 106 (1997) 5062.
[11] J.S. Cao, M. Messina, K.R. Wilson, J. Chem. Phys. 106 (1997) 5239.
[12] J.S. Cao, K.R. Wilson, Phys. Rev. A. 55 (1997) 4477.
[13] J.S. Cao, K.R. Wilson, J. Chem. Phys. 107 (1997) 1441.
[14] V.V. Yakovlev, C.J. Bardeen, J. Che, J.S. Cao, K.R. Wilson, J. Chem. Phys. 108 (1998) 2309.

[15] C.J. Bardeen, J. Che, K.R. Wilson, V.V. Yakovlev, V.A. Apkarian, C.C. Martens, R. Zadoyan, M. Messina, J. Chem. Phys. 106 (1997) 8486.
[16] Z. Li, J.Y. Fang, C.C. Martens, J. Chem. Phys. 104 (1996) 6919.
[17] R. Trebino, K.W. DeLong, D.N. Fettinghoff, J.N. Sweetser, M.A. Krumbugel, B.A. Richman, D.J. Kane, Rev. Sci. Instrum. 68 (1997) 3277.
[18] J.C. Diels, W. Rudolph, Ultrafast Pulse Phenomena, Academic Press, NY, 1996.
[19] R. Zadoyan, J. Almy, V.A. Apkarian, J. Chem. Soc. Faraday Disc. 108 (1997) 255.